Dexamethasone degradation in aqueous solution via photocatalytic UV/H_2O_2 /MgO process: kinetic studies

Ghorban Asgari
Hamadan University of Medical Sciences
Mehdi Salari
Hamadan University of Medical Sciences
Mohammad MollaMahmoudi
Hamadan University of Medical Sciences
Reza jamshidi
Hamadan University of Medical Sciences
Ali Dehdar
Hamadan University of Medical Sciences
Hossein Faraji (farajiehe@gmail.com)
Hamadan University of Medical Sciences
Solmaz Zabihollahi
Hamadan University of Medical Sciences
Saber Alizadeh
Hamadan University of Medical Sciences

Article

Keywords: MgO nanoparticles, Dexamethasone degradation, Hydrogen Peroxide, Photocatalytic process

Posted Date: June 14th, 2022

DOI: https://doi.org/10.21203/rs.3.rs-1673390/v1

Abstract

Wastewaters discharged from different industries and hospitals may contain pharmaceuticals, especially dexamethasone (DEX). Thus, we applied the UV/H_2O_2 photocatalytic method in the presence of the MgO nanoparticles to remove dexamethasone from synthetic wastewater. Moreover, the effects of parameters such as pH = 3–11, hydrogen peroxide concentration = 1–8 mM, initial DEX concentration (5–30 mg/L), catalyst dosage = 0.01–0.2 g/l were investigated at the contact times of 0–30 min. Furthermore, the efficiency of UV/H_2O_2 in the presence and absence of catalyst was investigated. Additionally, this catalyst was characterized by means of XRD and FT-IR analyses and SEM imaging. It was found that the removal rate was enhanced with decreasing pH and initial dexamethasone concentration. The removal rate was enhanced somewhat with concentrations of hydrogen peroxide and MgO. In the case of UV/H_2O_2/MgO, 87% removal efficiency achieved, under the optimal conditions: pH 3, contact time of 30 min, dexamethasone content of 20 mg/L, H_2O_2 of 0.5 mM, and UV radiation of 55 watts. The kinetic data indicated that the reaction followed the second-order kinetic model. The results showed that the UV/H_2O_2 photochemical process can efficiently remove dexamethasone from aqueous in the presence of MgO catalyst, and the mineralization efficiency was reached at about 98%.

Highlights

- UV/H_2O_2 with MgO nanoparticles is efficient for dexamethasone removal.
- UV, H_2O_2, and MgO act synergistically for dexamethasone removal.
- The reaction followed the second-order kinetic model.

1. Introduction

Over recent decades, huge quantities of effluent containing various contaminants have been discharged into water bodies. Pharmaceutical compounds, which are considered a group of emerging contaminants, can be entered into the environment after or even without consumption [1]. Genetic mutations and sexual disorders may be due to the presence of these compounds in water [2]. Corticosteroids, which are widely applied to treat human and animal diseases, are a large class of drugs. They are entirely non-biodegradable and are utilized to relieve inflammation in the human body. One of the most widely applied corticosteroids is dexamethasone (DEX) (Table 1). It is no wonder that wastewater produced by medical centers and hospitals contains a high content of this compound [3].

Table1 The characteristics of dexamethasone.

Chemical formula	$C_{22}H_{29}FO_5$
λ_{max}	254 nm
Molar mass	392.461 $g.mol^{1-}$
Chemical structure	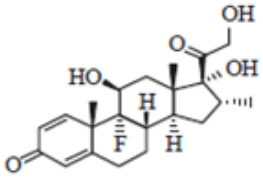

Many processes, like membrane bioreactors[4], carbon nanotubes [5] and anaerobic reactors [6], have been utilized to treat wastewater containing pharmaceuticals. It should be noted that processes such as electrical coagulation [2] and adsorption [7] have been used for dexamethasone. Biological treatment methods are time-consuming and a high volume of sludge is generated in the electrical coagulation process [2]. Moreover, adsorption is not a cost-effective method because of the high cost of waste disposal. The basis of the advanced oxidation processes (AOPs) is the generation of hydroxyl radicals capable of degrading persistent organic pollutants (POPs). Also, these methods have attracted much attention owing to their capability in the treatment of a wide range of organic materials, which cannot be degraded by conventional chemical and biological methods [8]. In general, strong oxidants like hydrogen peroxide and ozone are generated or methods like ultrasonic, electron beam, and so forth are applied [9]. Among various AOPs, the application of photocatalytic processes is increasingly considered due to the possibility of producing cost effective and eficient photocatalysts. In a photocatalytic reaction, a catalyst is exposed to visible or UV light irradiation for the generation of hydroxyl radicals. In photocatalytic processes, semiconductors like TiO_2, ZnO, CdS, and ZrO_2 have mainly been used for organic matter degradation [10]. In general, nanoparticles are suitable for chemical reactions and adsorption of different organic materials because of their high specific surface area [11]. Among these nanoparticles, MgO, which is a basic oxide, has various applications as a catalyst. Magnesium oxide (MgO) is a semiconductor whose unique chemical, mechanical, optical, and electrical properties,wide energy band gap, stability, inexpensiveness, and non-toxicity have made it very attractive for application in photocatalytic processes [12]. It has been observed that the use of the MgO nanoparticles in concert with catalytic ozonation can enhance the degradation of organic pollutants [13]. In this research, we tried to investigate the catalytic impact of MgO nanoparticles alongside UV radiation for hydrogen peroxide activation. Thus, in the presence of the MgO nanoparticles, the performance of the UV/H_2O_2 process in DEX removal from the aqueous environment was assessed.

2. Materials And Methods

2.1. Chemicals and Photoreactor

All the chemicals utilized in this study, H_2O_2, NaOH, and H_2SO_4, and radical scavengers: ascorbic acid (AA), ethylenediamine tetraacetic acid (EDTA), and tert-butyl alcohol (TBA), were purchased from Sigma Aldrich and

Merck Co., Germany. The MgO nanoparticle powder was purchased from ASPI Co. and sodium dexamethasone phosphate ($C_{22}H_{28}FNa_2O_8P$) was bought from Darou Pakhsh Pharmaceutical Co. For the tests, a 2-liter stainless steel photoreactor, which was equipped with quartz glass and a 55-watt low-pressure lamp (Philips Co), was employed for the tests. A pump was used in order to continuously mix the samples. Figure 1 presents all the details of the reactor.

2.2. Experimental Procedures

All experiments were performed in a batch-flow pilot. In the current research, at the fixed intensity of ultraviolet light, the impacts of pH of 3–11, the initial DEX content of 5, 10, 20, 30 mg/L, hydroxyl content of 1–8 mM, MgO dose of 0.01–0.2 g/L, and contact time of 0–30 min on the process performance were studied. All runs were carried out in triplicate at room temperature (25°C), and average figures were recorded. Both first- and second-order linear kinetics were used to obtain the best-fitting model for the removal process.In this work, a solution containing 100 mg/l of the pollutant was prepared. Next, the working concentrations were prepared from this stock solution. A UV/Vis spectrophotometer (wavelength = 241 nm) (DR 5000, Hach Co., Germany) was employed to determine the contents of the DEX solution. Furthermore, as superoxide anion ($^{\bullet}O_2$), hole (h^+), and hydroxyl radical ($^{\bullet}OH$), AA (0.2 mol/L), EDTA (0.2 mol/L), and TBA (0.2 mol/L) were used, respectively. In order to determine the mineralization rate of the pollutant during the process, the total organic carbon (TOC) of the experiments was detected using a Shimadzu 5000 TOC analyzer. Moreover, the chemical oxygen demand (COD) was determined according to the procedure expressed in Standard Methods (Federation & Association). A digital pH meter (Hach) was applied to determine the pH values. In the end, all the charts were plotted and the data was analyzed by means of Excel 2013.X-ray Powder Diffraction (XRD) was used to determine the crystal phases of the MgO nanoparticles (Rigaku Ultima IV). The morphologies of the catalyst surface were evaluated using Field Emission Scanning Electron Microscopy (FE-SEM; FEI Nova NanoSEM 450). Moreover, Fourier-transform infrared spectroscopy (FTIR) (Thermo, AVATAR) using a pellet generated by integrating the powder sample with KBr was used to observe functional groups of MgO nanoparticles.

3. Results And Discussion

3.1. The characterization of the catalyst

Figure 2 presents the morphological properties of the nanoparticles as determinedby the scanning electron microscopy (SEM) analysis, performed before starting the reaction. As can clearly be seen, it is obvious that the magnesium oxide nanoparticles had a porous, spongy structure. Figure 3 illustrates, in the amorphous, shape, two peaks seen in 2θ = 43 and 62, illustrating the presence of cubic MgO, and the peaks can be assigned to a pure phase of MgO. The FTIR spectrum was also tested for investigation and identification of the catalyst surface's functional groups. It is well known that MgO chemisorbs H_2O and CO_2 molecules from the atmosphere due to its surface acid–base properties [14]. The major peaks appearing in the FT-IR spectra may be assigned to the following vibrational modes: (i) –OH stretching vibrations of the surface bonded (or) adsorbed water, (ii) –OH stretching vibrations of structural water corresponding to M-OH stretching, (iii) –OH bending vibrations of structural water, corresponding to M-OH bending, and (iv) Mg–O vibrations. As can be seen from Fig. 4, the peaks at 3440 and 1629 cm^{-1} are assigned to -OH stretching bands and -OH bending vibrations, respectively, of physically adsorbed water molecules and surface hydroxyl groups strongly perturbed by hydrogen bonding. The surface hydroxyl groups have been recognized to play an important role in the photocatalytic reaction since they can inhibit the

recombination of photogenerated charge carriers, and also interact with the photogenerated holes to produce active oxygen specie [15].

3.2. Impact of Initial pH

The literature review revealed that AOPs are completely pH-dependent [16]. Hence, in this study, at the fixed hydroxyl content of 1 mM, the pH values were changed from 3 to 11 to investigate the changes in the removal efficiency. The maximum removal efficiency (73%) by the UV/H_2O_2/MgO method was attained at a pH of 3 (Fig. 5). These findings are attributed to the surface properties of the adsorbent and the ionization/degradation of the adsorbate. The number of H^+ increases gradually with decreasing pH. When H^+ is adsorbed, the positive charge on the nanoparticle's surface increases and, in turn, the electrostatic force between the cationic charge on the surface of the nanoparticle and the negative DEX molecule enhances, resulting in an increase in the adsorption rate. It was found that the performance declined sharply when pH was raised. For example, a 45% decrease was seen in removal efficiency at a pH value of 11 within 30 min. As can be seen, the degradation rate remained unchanged after 20 min and was insignificant after 30 min. Therefore, reaction times of between 0 and 30 min were selected for the rest of the experiments. Furthermore, a decrease in the removal efficiency of the H_2O_2/UV in alkaline conditions can be caused by a reaction between H_2O_2 and solution alkalinity; this causes hydroxyl radicals to go down. Moreover, in comparison with neutral pH, the nanoparticles are accumulated in acidic conditions; as a result, the catalyst's effective surface area is enhanced [17].

3.3. Impact of H_2O_2 dosage

In this study, under the following conditions: at pH 3, with DEX content of 20 mg/L and catalyst dosage of 0.05 g/L, different initial contents of hydroxyl (1–8 mM) were tested. The results have been presented in Fig. 6. Apparently, when the concentration of H_2O_2 was raised, the removal efficiency went up to 87%. It should be noted that, when the H_2O_2 concentration exceeded 5 mM, the removal efficiency started to decline. An excessive increase in H_2O_2 concentration causes part of °OH to be inhibited and then HO_2 is produced, which has a lower oxidation potential than °OH (Eq. (1)) [18]. Also, this decrease in performance can be because of continuous degradation of H_2O_2 into oxygen and water.

$H_2O_2 + OH^{\bullet} \rightarrow H_2O + HO_2^{\bullet}$ (1)

3.4. Impact of initial DEX concentration

In photocatalytic processes, how the initial concentration of the pollutant affects the removal efficiency is of great importance. Figure 7 shows the impact of initial DEX content on the removal efficiency in UV/H_2O_2/MgO. As can be seen, with an increasing DEX concentration from 5 to 30 mg/L, the removal efficiency declined. And, 65% of DEX was degraded at a concentration of 30 mg/L. Within 5 min of the reaction and an initial DEX content of 5 mg/L, a 90% removal efficiency was reached (Fig. 7). The decrease in the removal rate by increasing the concentration of DEX can be attributed to the fact that at all concentrations, the amount of nanoparticles, contact time, and pH are the same. As a result, the amount of radicals produced is similar at all four concentrations. Naturally, it is expected to see lower DEX degradation at lower concentrations. By contrast, at a lower initial concentration, the number of active sites on the catalyst’s surface capable of degrading DEX increases. Furthermore, ultraviolet light cannot penetrate effectively into the solution when there are higher concentrations of DEX [19].

3.5. Impact of the dose of MgO

In Fig. 8, howthe changes in magnesium oxide (0.01 to 0.2 g/l) affected the removal efficiency of the pollutant in photo-oxidation has been shown. As can be seen, the removal efficiency went up with the raising of the dose of MgO. Nevertheless, when the dosage exceeded 0.05 g/l, the removal rate declined. At higher dosages, there are more active sites and free electrons in the conductor, resulting in the generation of more hydroxyl radicals that can take part in degradation [20]. Also, the removal rate of DEX at higher dosages of this nanoparticle was marginal, because the nanoparticles stuck together, causing the intensity of the UV lamp to decrease. Sobana et al. reported that during the photocatalytic reactions, the removal efficiency of Red Direct 23 increased as an increase in the number of active sites, resulted from a rise in the dosage of titanium dioxide doped with silver [21]. It should be noted that the current study's findings are consistent with those of other related studies [12].

3.6. Impact of radical scavengers

In this study, the main reactive species in DEX degradation were identified using radical scavenging experiments under optimal conditions. To investigate the effects of different scavengers on DEX degradation, AA (0.2 mol/L), EDTA (0.2 mol/L), and TBA (0.2 mol/L) were added to the DEX solution as superoxide anion (•O2), hole (h+), and hydroxyl radical (•OH) scavengers, respectively [22]. The results show three types of inhibition, corresponding to the three active species in the UV/H_2O_2/MgO process. From Fig. 9, 87% of DEX can be removed in 30 min without a scavenger (Control). However, with the addition of AA, EDTA, and TBA, DEX removal efficiency decreased to 73.5%, 64.6%, and 34.8%, respectively (Fig. 9). Since TBA is a known ˙OH scavenger [23], the DEX degradation in the established UV/H_2O_2/MgO system in the presence of TBA clearly shows that the reaction with ˙OH was the predominant active specie contributing to DEX removal. This result corresponds with Akbari et al., [24] study that stated hydroxyl radicals are the main mechanism in ciprofloxacin antibiotic removal using S, N-doped MgO nanoparticles under UVA-LED.

3.7. TOC analysis and Mineralization

In this study, the content of TOC was determined because DEX is initially converted to other degradation byproducts thatare still organic. Thus, we determined the mineralization of DEX through recording TOC concentrations over the process. The TOC and COD concentrations of the samples were determined under the selected conditions (Fig. 10). It was found that the initial TOC was determined at 53.8 mg/L, and it declined to 23.5 mg/L after the exertion of the UV/H_2O_2/MgO process for 30 min, illustrating a mineralization rate of 56%. Accordingly, COD was reduced by up to 65%. However, at the same contact time, the rate of DEX removal was 87%. Thus, it is claimed that for more mineralization, more contact time is required. For instance, the TOC removal rate increased to 98% within 120 min. It should be pointed out that lower by-products can be generated when a suitable contact time is regarded for reaching the mineralization rate of interest by means of the UV/H_2O_2/MgO process. It should be noted that, in the application of photocatalytic reactions, intermediates must be detected and eco-toxicological examinations should be performed.

3.8. Comparison of the processes

In this study, the UV/H202 process was run in the presence and absence of the MgO catalyst.Also, the results of the UV and UV/MgO processes were compared. As indicated in Fig. 11, only 8% of the pollutant was degraded via the UV application within 30 min. And, the performance of the UV/MgO process was nearly 17%, which may be because of the low adsorption rate that occurred on the surface of magnesium oxide. It should be noted that there was a dramatic difference between the removal efficiency rates of the UV/H_20_2 photo-oxidation and the UV/H_20_2/MgO process, which were found to be61% and 87%, respectively. The activity of magnesium oxide in

catalyzing oxidation decay was relative to the surface acid–base properties of the oxide. Water molecules can be adsorbed on the magnesium oxide**'s** surface due to the unsaturated state of surface electrons. As a result, surface hydroxyl groups may be formed. These groups play a basic role in the acid–base characterizations of magnesium oxide. Therefore, the process can be catalyzed well due to the surface hydroxyl groups. Thus, it is expected to see more DEX removal in the presence of magnesium oxide.

3.9. Investigation of process Kinetics

The behavior of DEX removal was studied by both the linear forms of pseudo-first and second-order kinetic models [25] as expressed in Eqs. 2 and 3.

$$Ln_{Ct} = Ln_{C0} \times e^{-kt}$$

2

$$\frac{1}{Ln_{Ct}} = \frac{1}{Ln_{C0}} + k_2 t$$

3

Here, C_0 and C_t show DEX concentration at times 0 and t (min), respectively. k_1 (min^{-1}) and k_2 (mg/L.min) are assigned to the first and second order kinetic constants, respectively. Figures 12 and 13 show pseudo first and second-order kinetic models obtained by plotting Ln (c_t/c_0) and $1/c_t – 1/c_0$ against reaction time. The values of k_1 and k_2 obtained in accordance with the corresponding kinetic models are given in Table 2. In addition, the R^2 values for all the single, binary, and ternary processes are better fitted to the pseudo-second-order kinetic model. The findings strongly indicate that the reaction constant for the UV/H_2O_2/MgO process was the highest among other methods of DEX removal. This illustrates that the combined UV/H_20_2/MgO methods were more effective in DEX removal than

Table 2
The obtained coefficients of first and second order kinetic models for the removal of DEX by UV, MgO, UV/H2O2 and UV/H2O2/MgO processes were calculated.

Process	UV		MgO		UV/MgO		UV/H_2O_2		UV/H_2O_2/ MgO	
	R^2	K	R^2	K	R^2	K	R^2	K	R^2	K
First-order model	0.9704	0.0071	0.9261	0.0077	0.9689	0.0178	0.8456	0.0333	0.8782	0.0774
Second –order model	0.977	0.0008	0.9394	0.0009	0.9824	0.0023	0.9239	0.0057	0.9804	0.0279

4. Conclusion

In this study, dexamethasone was degraded by using H_2O_2 and hydroxyl radical generation-based AOP processes. It was found that, with decreasing pH and initial DEX concentration, the removal efficiency of the UV/H_2O_2/MgO

method improved. Also, the following values were determined to be the optimum conditions: hydroxyl and magnesium oxide nanoparticle concentrations up to 5 Mm and 0.05 gr/L, initial concentration of 20 mg/l, and contact time of 30 min. The kinetic response illustrated that the obtained data followed the pseudo-first order kinetic model. The findings also indicated that the UV/H_2O_2 method could dramatically degrade the pollutant from an aqueous solution when the MgO catalyst was applied as a catalyst (mineralization rate of 98%). Further, the catalytic activity of magnesium oxide is attributed to the surface acid-base characterization of this oxide. By large, the used process can be considered a suitable method for the removal of pharmaceuticals under optimum conditions.

Declarations

Acknowledgement

Sincere thanks and appreciation goto Hamadan University of Medical Sciences and the experts of the Faculty of Water and Wastewater Laboratory for their financial support and help in conductingthis research.

Availability of Data and Materials

All data generated or analysed during this study are included in this published article.

References

1. Santos, L.H., et al., *Ecotoxicological aspects related to the presence of pharmaceuticals in the aquatic environment*. Journal of hazardous materials, 2010. **175**(1–3): p. 45–95.
2. Arsand, D.R., K. Kümmerer, and A.F. Martins, *Removal of dexamethasone from aqueous solution and hospital wastewater by electrocoagulation*. Science of the Total Environment, 2013. **443**: p. 351–357.
3. Mohseni, S., et al., *Removal of dexamethasone from aqueous solutions using modified clinoptilolite zeolite (equilibrium and kinetic)*. International journal of environmental science and technology, 2016. **13**(9): p. 2261–2268.
4. Deegan, A., et al., *Treatment options for wastewater effluents from pharmaceutical companies*. International Journal of Environmental Science & Technology, 2011. **8**(3): p. 649–666.
5. Wang, J. and S. Wang, *Removal of pharmaceuticals and personal care products (PPCPs) from wastewater: a review*. Journal of environmental management, 2016. **182**: p. 620–640.
6. Chelliapan, S., et al., *Influence of organic loading on the performance and microbial community structure of an anaerobic stage reactor treating pharmaceutical wastewater*. Desalination, 2011. **271**(1–3): p. 257–264.
7. Ahmed, M.J., *Adsorption of non-steroidal anti-inflammatory drugs from aqueous solution using activated carbons*. Journal of environmental management, 2017. **190**: p. 274–282.
8. Shokoohi, R., et al., *Investigation of the efficiency of heterogeneous Fenton-like process using modified magnetic nanoparticles with sodium alginate in removing Bisphenol A from aquatic environments: kinetic studies*. 2018. **101**: p. 185–192.
9. Moghaddam, S.K., et al., *Removal of tylosin from aqueous solution by UV/nano Ag/S 2 O 8 2 − process: Influence of operational parameters and kinetic study*. Korean Journal of Chemical Engineering, 2014. **31**(9): p. 1577–1581.

10. Khattab, I.A., et al., *Photocatalytic degradation of azo dye Reactive Red 15 over synthesized titanium and zinc oxides photocatalysts: a comparative study*. 2012. **48**(1–3): p. 120–129.
11. Shokoohi, R., et al., *Effective Removal of Azo Dye Reactive Blue 222 from Aqueous Solutions Using Modified Magnetic Nanoparticles with Sodium Alginate/Hydrogen Peroxide*. 2019. **38**(s1): p. S205-S213.
12. Jorfi, S., et al., *Enhanced coagulation-photocatalytic treatment of Acid red 73 dye and real textile wastewater using UVA/synthesized MgO nanoparticles*. 2016. **177**: p. 111–118.
13. Bahrami-asl, F., et al., *Catalytic ozonation of azo dye reactive red 120 in the presence of MgO nanoparticles.* 2017.
14. Mageshwari, K., et al., *Template-free synthesis of MgO nanoparticles for effective photocatalytic applications*. 2013. **249**: p. 456–462.
15. Mageshwari, K., et al., *Template-free synthesis of MgO nanoparticles for effective photocatalytic applications*. Powder technology, 2013. **249**: p. 456–462.
16. Shookohi, R., et al., *The efficiency of UV/S2O82 − photo-oxidation process in the presence of Al2O3 for the removal of dexamethasone from aqueous solution: kinetic studies*. 2019. **79**(5): p. 938–946.
17. French, R.A., et al., *Influence of ionic strength, pH, and cation valence on aggregation kinetics of titanium dioxide nanoparticles*. Environmental science & technology, 2009. **43**(5): p. 1354–1359.
18. Jaafarzadeh, N., et al., *The performance study on ultrasonic/Fe3O4/H2O2 for degradation of azo dye and real textile wastewater treatment*. 2018. **256**: p. 462–470.
19. Modirshahla, N. and M.A. Behnajady, *Photooxidative degradation of Malachite Green (MG) by UV/H2O2: Influence of operational parameters and kinetic modeling*. Dyes and Pigments, 2006. **70**(1): p. 54–59.
20. Quan, X., et al., *Photoelectrocatalytic degradation of pentachlorophenol in aqueous solution using a TiO2 nanotube film electrode*. 2007. **147**(2): p. 409–414.
21. Sobana, N., et al., *Optimization of photocatalytic degradation conditions of Direct Red 23 using nano-Ag doped TiO2*. 2008. **62**(3): p. 648–653.
22. Dehdar, A., et al., *Step-scheme BiVO4/WO3 heterojunction photocatalyst under visible LED light irradiation removing 4-chlorophenol in aqueous solutions*. Journal of Environmental Management, 2021. **297**: p. 113338.
23. Asgari, G., et al., *Mineralization, kinetics, and degradation pathway of pentachlorophenol degradation from aqueous media via persulfate/dithionite process*. Arabian Journal of Chemistry, 2021. **14**(10): p. 103357.
24. Akbari, S., G. Moussavi, and S. Giannakis, *Efficient photocatalytic degradation of ciprofloxacin under UVA-LED, using S, N-doped MgO nanoparticles: synthesis, parametrization and mechanistic interpretation*. Journal of Molecular Liquids, 2021. **324**: p. 114831.
25. Yari, K., et al., *A comparative study for the removal of imidacloprid insecticide from water by chemical-less UVC, UVC/TiO 2 and UVC/ZnO processes*. Journal of Environmental Health Science and Engineering, 2019: p. 1–15.

Figures

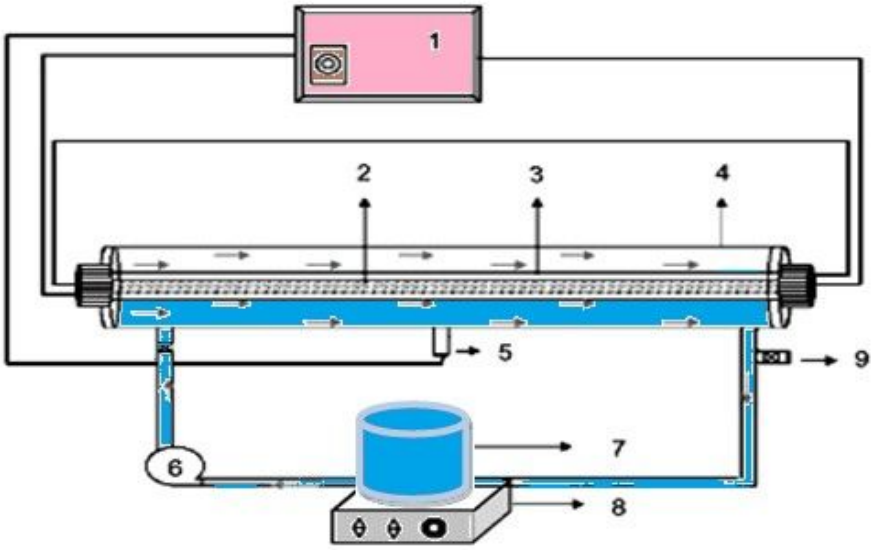

Figure 1

A schematic diagram of the reactor: (1) transformer, (2) low-pressure mercury-vapor UV lamp, (3) quartz cover (L: 85 cm D: 5 cm), (4) stainless steel box (L:85 cm D: 8 cm) , (5) photocell, (6) pump (50–400 ml/min), (7) beaker (2 Liters), (8) shaker, and (9) sampling tube.

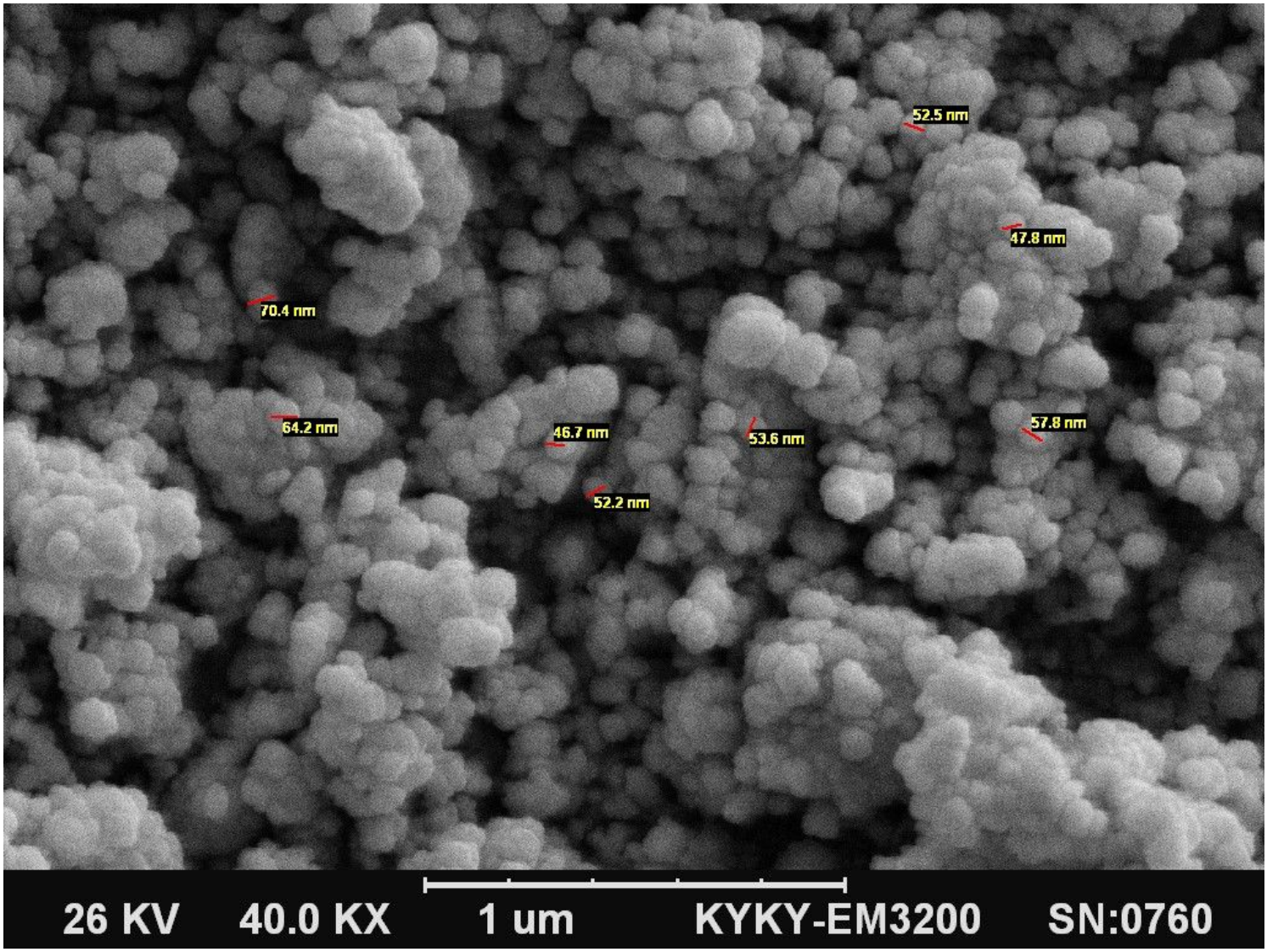

Figure 2

Scanning Electron Microscope (SEM) image of the MgO nanoparticles

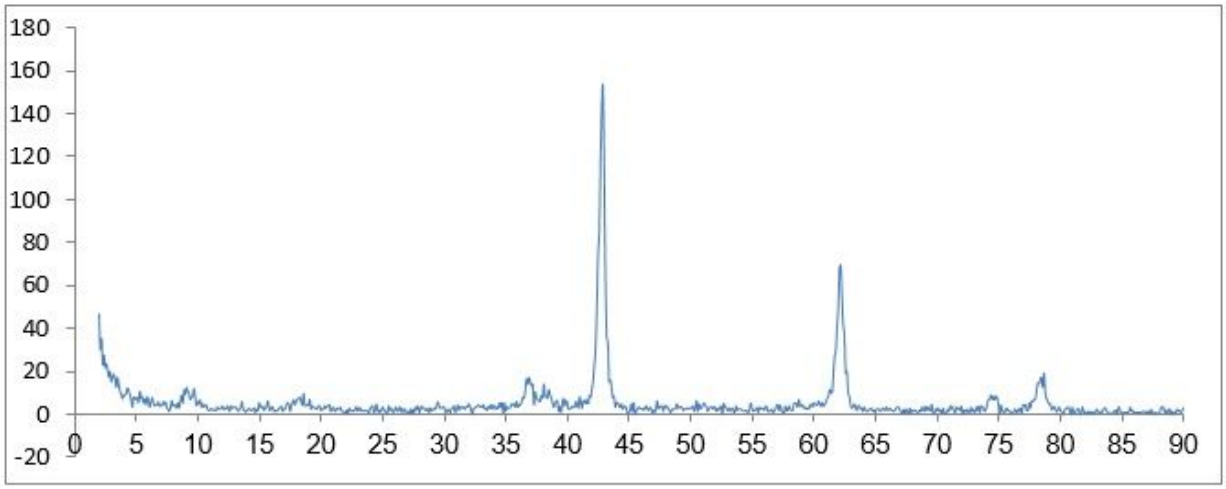

Figure 3

XRD analysis of the MgO nanoparticles.

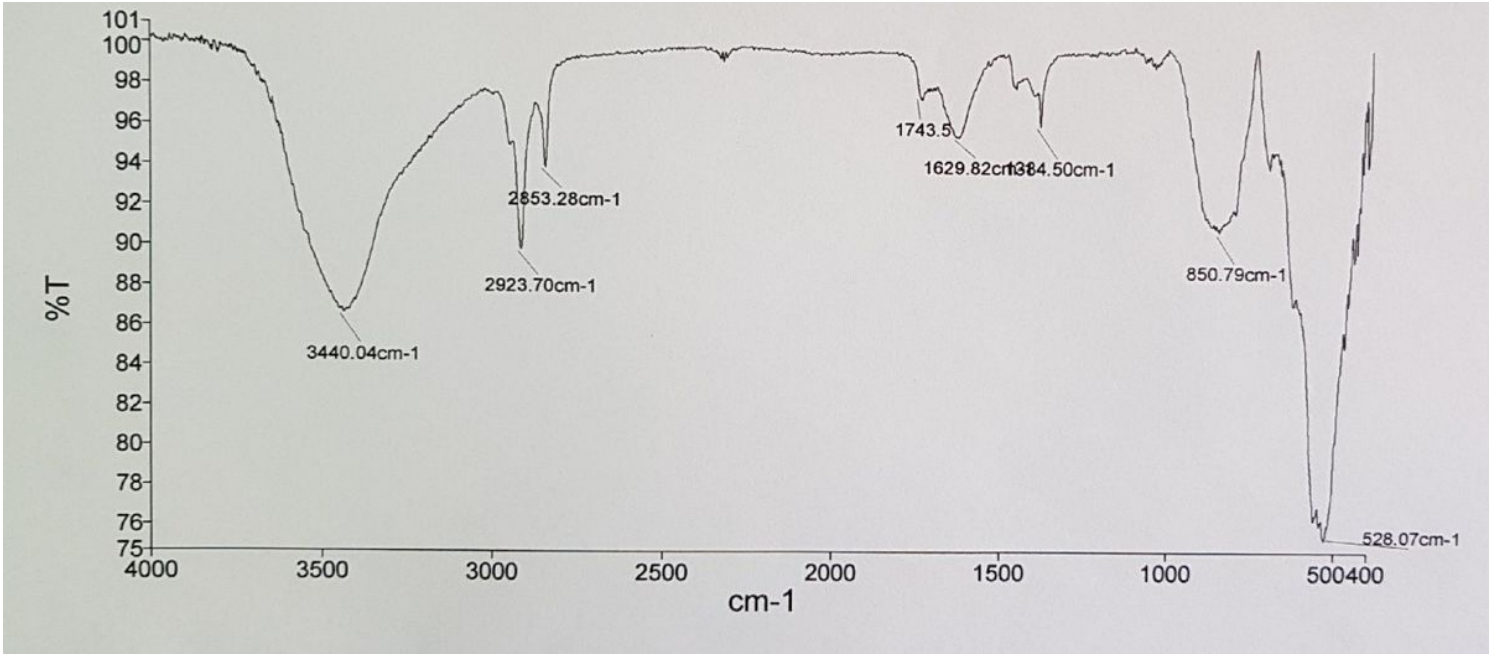

Figure 4

FTIR spectra of the MgO nanoparticles

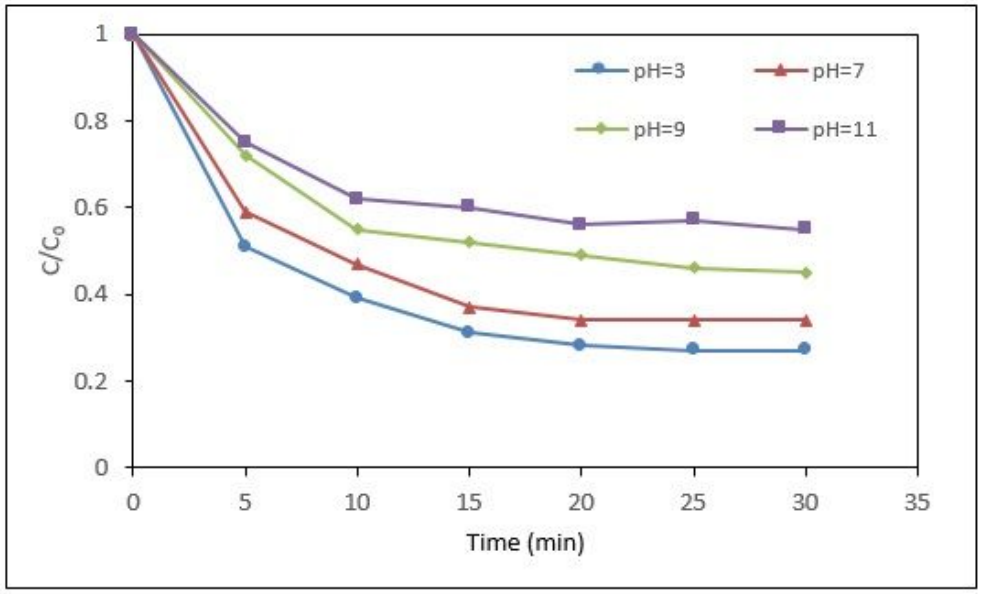

Figure 5

Impact of pH on DEX degradation: hydroxyl dosage = 1mM, DEX content = 20mg/L, and MgO dosage = 0.05g/L).

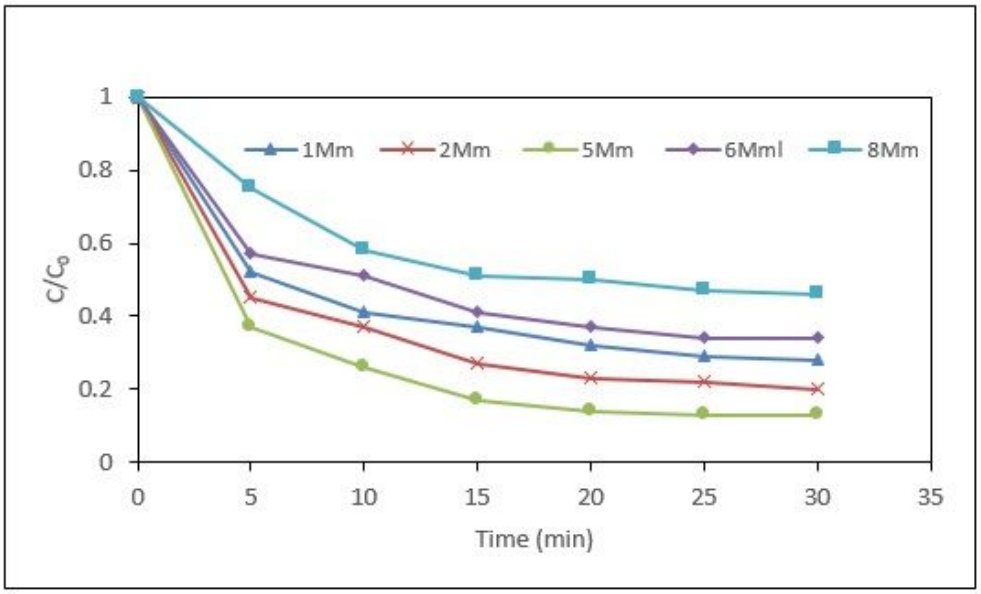

Figure 6

Impact of H_2O_2 dosage on the removal efficiency of DEX under the following conditions: pH = 3, DEX concentration = 20 mg/L and MgO dosage = 0.05 g/L.

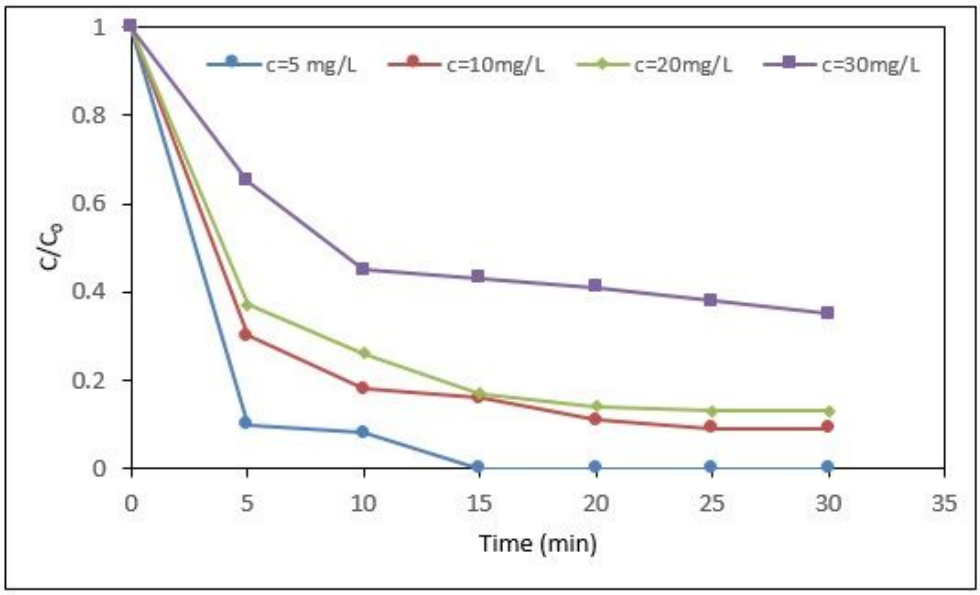

Figure 7

Impact of initial DEX content on DEX removal rate: pH = 3, hydroxyl dose =5 mM and MgO dose = 0.05g/L.

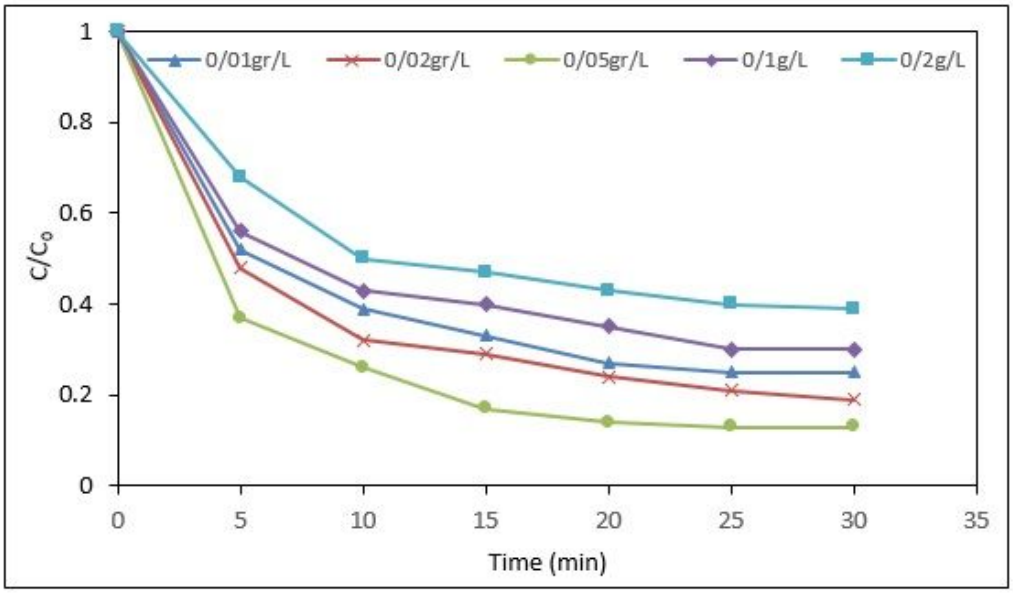

Figure 8

Impact of MgO dose on the rate of DEX removal: initial dexamethasone content = 20 mg/L, pH = 3, and hydroxyl dosage = 5 mM.

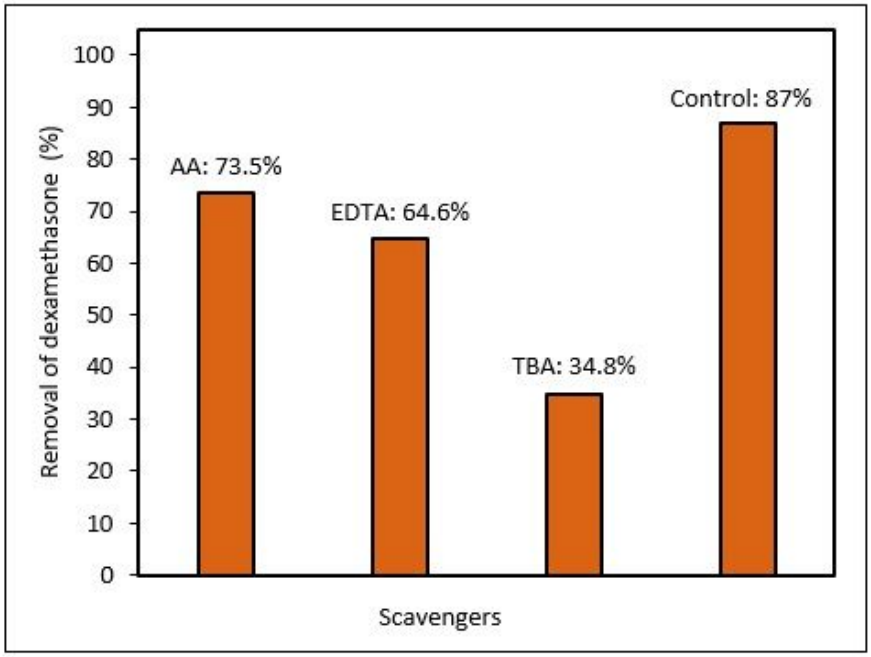

Figure 9

The degradation rate of DEX in the presence of different radical scavengers (initial DEX concentration = 20 mg/L, pH = 3, H_2O_2 dose = 5 mM, and MgO dose = 0.05 g/L).

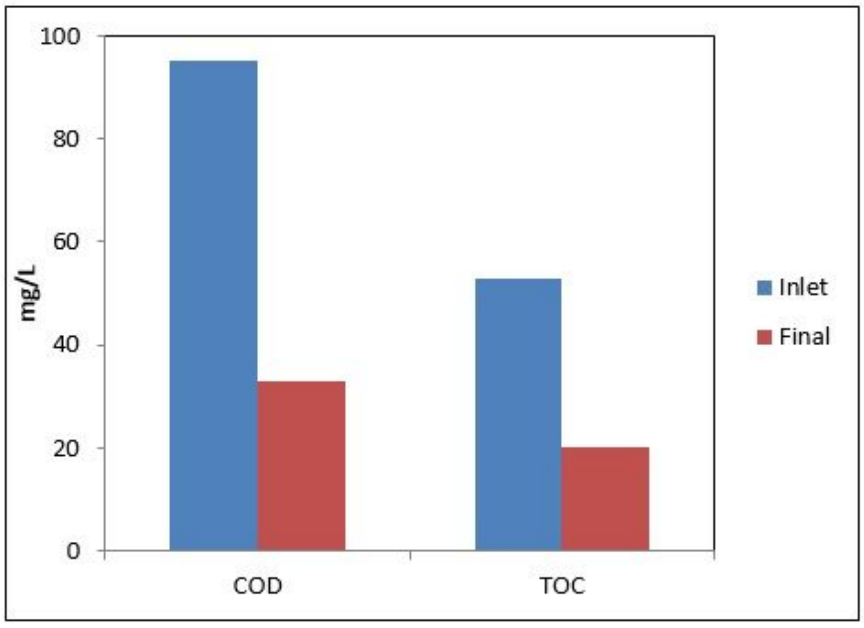

Figure 10

TOC and COD removal (initial DEX concentration = 20mg/L, pH = 3, H_2O_2 dose = 5 mM, andMgO dose = 0.05 g/L).

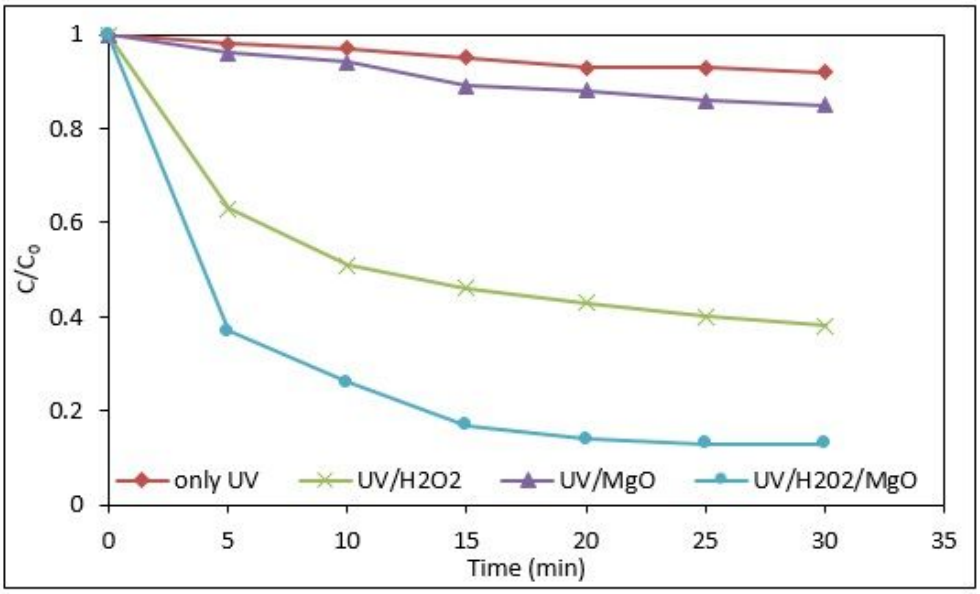

Figure 11

Comparison of the UV, UV/H_2O_2, UV/MgO and UV/H_2O_2/MgO processes under the optimum conditions.

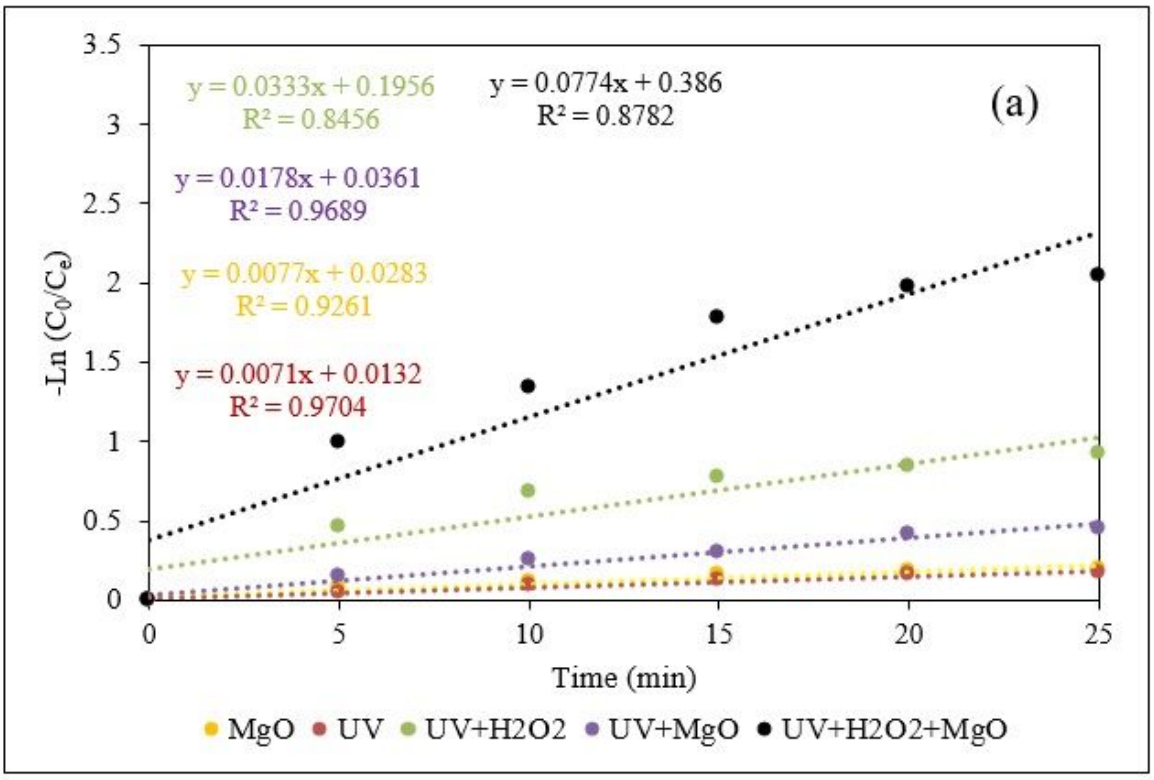

Figure 12

Based on a pseudo-first-order model, the degradation behavior of DEX in the processes MgO, UV, UV+H_2O_2+UV+MgO, and UV+H_2O_2+MgO was studied.

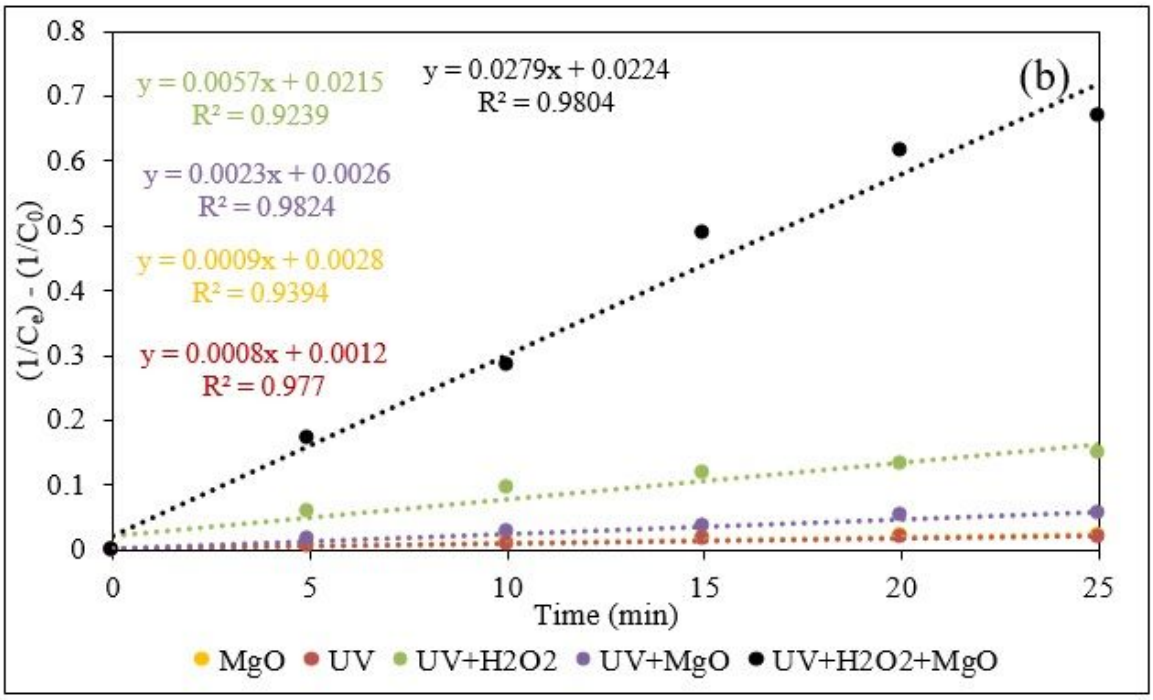

Figure 13

Based on a pseudo-second-order model, the degradation behaviour of DEX in the processes MgO, UV, UV+H_2O_2+UV+MgO, and UV+H_2O_2+MgO.